Oxidized Pea Starch/Chitosan Composite Films: Structural Characterization and Properties

Haixia Wu,[1] Changhua Liu,[1] Jianguang Chen,[1] Yun Chen,[2,3] Debbie P. Anderson,[2] Peter R. Chang[2,4]

[1]*College of Chemistry and Chemical Engineering, Southwest University, 400715 Chongqing, China*
[2]*Bioproducts and Bioprocesses National Science Program, Agriculture and Agri-Food Canada, Saskatoon, SK S7N 0X2, Canada*
[3]*Research Centre for Medical and Structural Biology, School of Basic Medical Science, Wuhan University, Wuhan 430071, China*
[4]*Department of Agricultural and Bioresource Engineering, University of Saskatchewan, Saskatoon, S7N 5A9 SK, Canada*

Received 11 November 2009; accepted 3 May 2010
DOI 10.1002/app.32753
Published online 1 July 2010 in Wiley InterScience (www.interscience.wiley.com).

ABSTRACT: In this article, a series of oxidized pea starch/chitosan (OPS/CS) blend films were prepared by a casting and solvent evaporation method. The structure, thermal behavior, and mechanical properties of the films were investigated by means of Fourier transform infrared spectroscopy, wide-angle X-ray diffraction, scanning electron microscopy, thermogravimetric analysis, and tensile testing. The results suggested that, in addition to hydrogen bonding, the interactions between OPS and CS molecules were enhanced by the formation of electrostatic interaction between the negatively charged carboxyl groups on OPS and the positively charged amino groups on CS. Compared with the pea starch/chitosan (PS/CS) blend films, OPS/CS blend films exhibited significantly higher tensile strength with significantly lower elongation at break. Moreover, incorporation of CS into the OPS matrix also led to a decrease in moisture uptake by the composite film. © 2010 Wiley Periodicals, Inc. J Appl Polym Sci 118: 3082–3088, 2010

Key words: biodegradable; biopolymers; chitosan; composites; polysaccharides

INTRODUCTION

With severe environmental pollution caused by petroleum-based polymer materials and an inevitable increase in the price of petroleum, it is genuinely urgent for today's society to develop eco-friendly materials from renewable resources.[1] Among the many kinds of renewable polymers, starch has shown promise for applications in the fields of agriculture, industry, food engineering, and medicine in biodegradable plastics,[2] composites,[3] edible films,[4] food hydrocolloids,[5] surface coatings,[6–8] and packaging materials, and for drug delivery.[9] However, the commercialization of starch-based films/composites has been stagnant, primarily due to their poor mechanical properties and high moisture sensitivity.[10] Over the past decade, several strategies, including starch modification and blending with synthetic or natural polymers, have been explored by researchers but only with limited success.

One strategy worth exploring further is the blending of two distinct biopolymers to obtain composite materials in which each component provides a specific functional property.[11] Chitosan (CS) is derived from chitin, which is the second most abundant polysaccharide on earth, next to cellulose and is available from waste products of the shellfish industry.[12] CS is nontoxic, biodegradable, and biofunctional and has the structure of a linear copolymer with glucosamine and *N*-acetyl glucosamine units linked by β-1,4 glycoside. In an acidic environment, the amino group (NH_2) can be protonated to NH_3^+ to readily form electrostatic interactions with anionic groups. As expected, the functional properties of CS films are improved when CS is combined with other film-forming materials. For example, Hoagland and Parris prepared CS-pectin laminated films by interaction of the cationic groups of CS with the anionic groups of pectin.[13] Hosokawa et al. reported that when biodegradable films were made from CS and homogenized cellulose, previously oxidized with ozone, the mechanical properties of the films increased owing to the number of carbonyl and carboxyl groups from cellulose interacting with the CS amino groups.[14]

We have attempted to make full use of these two renewable and functional ingredients (i.e., starch

Correspondence to: P. R. Chang (peter.chang@agr.gc.ca).
Contract grant sponsors: Program of Energy Research and Development (PERD) of Natural Resources Canada, Pulse Research Network (PURENet), Agriculture and Agri-Food Canada's Agriculture Bioproducts Innovation Program (ABIP).

TABLE I
Codes for PS/CS and OPS/CS Blend Films

CS content (%)	0	10	30	50	70	90	100
PS/CS-*n*	PS/CS-0	PS/CS-10	PS/CS-30	PS/CS-50	PS/CS-70	PS/CS-90	PS/CS-100
OPS/CS-*n*	OPS/CS-0	OPS/CS-10	OPS/CS-30	OPS/CS-50	OPS/CS-70	OPS/CS-90	OPS/CS-100

and CS) for the preparation of novel, all-natural biocomposites. It is hypothesized that the newly introduced carboxyl groups in oxidized starch will improve the performance of oxidized starch and CS composite films. In this work, the carboxyl group was successfully introduced onto the glycosyl residues of pea starch through oxidation. The objective of this study was to prepare composite films from oxidized pea starch (OPS) and CS. The structure, thermal, and mechanical properties of the blend films were studied by Fourier transform infrared spectroscopy (FTIR), wide-angle X-ray diffraction (XRD), scanning electron microscopy (SEM), thermogravimetric analysis (TGA), and tensile testing. The relationship between the structure and functional properties of the OPS/CS blend films was also discussed.

EXPERIMENTAL

Materials

The raw material used in this study, field pea starch composed of 35% amylose and 65% amylopectin, was supplied by Nutri-Pea Limited Canada (Portage la Prairie, Canada). Chitosan (CS), with a weight-average molecular weight (M_w) of 3.0×10^5 and a degree of deacetylation greater than 90%, was purchased from Nantong Xincheng Biological Industrial Limited Co. China. Glycerol (99%), potassium permanganate (analytical grade), sulfuric acid (95–98%), and acetic acid (36%) were obtained from Maoye Chemical Co. (Chongqing, China).

Oxidized starch preparation and determination of degree of oxidation

The method of Huang et al.[15] was modified and used for the starch oxidation. A 40% (w/w) starch slurry (total weight 175 g) was stirred in a water bath. When the slurry temperature reached 50°C, 2.5 mL of 3*M* H_2SO_4 and 12.5 mL of 2% $KMnO_4$ were added and the mixture stirred at the same temperature until the color changed to milky white (about 2 h). The oxidized starch was filtered and washed 10 times with distilled water, and then dried at 40°C in a forced air oven for 24 h. The carboxyl content (degree of oxidation) of the resulting OPS was determined, according to the procedure of Chattopadhyay et al.,[16] to be 0.0945 %.

Film preparation

Different films were prepared by incorporating OPS, CS, and glycerol (30% total dried weight of OPS and CS). OPS solution (5 wt %) was prepared by dispersing 8 g of OPS powder and 24 mL of 10% glycerol in 136 mL purified water. The aqueous OPS suspension was stirred at 100°C in a water bath for 30 min until the solution became transparent and the OPS paste was obtained. The same volume (136 mL) of purified water was added to the OPS paste to avoid gelation. Meanwhile, 8 g CS powder and 24 mL 10% glycerol were added to 536 mL 2% (v/v) acetic acid and the mixture was stirred to form a transparent 1.4 wt % CS solution. The OPS and CS solutions were blended together to form a homogenous OPS/CS solution. The blended solutions were cast into plexiglass plates placed on a flat, level surface and dried in an oven at 40°C for 12 h. The dried films were then peeled off of the plates. By adjusting the CS content in the plasticized film to 0, 10, 30, 50, 70, 90, or 100 wt %, a series of OPS/CS blend films with a thickness of around 0.15 mm was prepared and coded as OPS/CS-*n*, where *n* was the percent of CS in the plasticized film. For example, the film coded as OPS/CS-10 has a CS content of 10 wt % in the solid composition. To serve as experimental controls, PS/CS blend films (coded as PS/CS-*n*, where *n* was the percent of CS in the plasticized film) were prepared using the same fabrication process. Codes for all films are listed in Table I. Before various characterizations, the resulting films were kept in conditioning desiccators of RH 43% at room temperature for more than 1 week to ensure equilibration of water in the films.

CHARACTERIZATION

Fourier transform infrared spectroscopy

FTIR spectra of the blend films in the attenuated total reflection mode were recorded with a Nicolet (USA) 170SX Fourier transform infrared spectrometer in the wavelength range of 4000–650 cm^{-1}.

X-ray diffractometry

XRD patterns of the samples were analyzed on a XRD-3D, PuXi (Beijing, China) X-ray diffractometer under the following conditions: Nickel filtered CuKα radiation ($\lambda = 0.15406$ nm) at a voltage of 36 kV and

current of 20 mA. The scanning rate was 4°/min in the angular range of 5°–30° (2θ).

Scanning electron microscopy

The blend films were fractured in liquid nitrogen and the cross-sections mounted on SEM stubs with double sided adhesive carbon tape, and then coated with gold under a vacuum of 13.3 Pa. A scanning electron microscope (S-4800, Hitachi, Japan) was used to observe the morphologies of the sample cross-sections at an accelerating voltage of 0.5 kV.

Thermogravimetric and differential thermogravimetric analysis

Thermogravimetric (TG) and differential thermogravimetric (DTG) analysis of OPS/CS blend films were carried out on a TA-STD**Q60**0 (TA Instruments Inc., New Castle, USA). The thermograms were acquired between 20 and 500°C at a heating rate of 10°C/min. Nitrogen was used as the purge gas at a flow rate of 20 mL/min. An empty Al_2O_3 pan was used as a reference.

Mechanical properties

The tensile strength and elongation at break of the films were determined using a Micro-electronics Universal Testing Instrument Model Sansi 6500 (Shenzhen Sans Test Machine Co., Shenzhen, China) according to the Chinese standard method (GB 13,022-91). The films were cut into 10 mm wide and 100 mm long strips and mounted between cardboard grips (150 mm × 300 mm) using adhesive so that the final area exposed was 10 mm × 50 mm. The cross-head speed was 10 mm/min. All measurements were performed on three specimens and averaged.

Moisture uptake test

The moisture uptake (MU) of the OPS/CS blend films was determined following the published method of Xu et al.[17] The samples used were thin rectangular strips with dimensions of 50 mm × 10 mm × 0.1 mm. They were vacuum-dried at 80°C overnight and then kept at 0% RH (P_2O_5) for 1 week. After weighing, the samples were conditioned at room temperature in a desiccator of 92% RH (Na_2CO_3 saturated solution). The MU of the samples was calculated as follows:

$$MU = (W_1 - W_0)/W_0 \times 100\%$$

where W_0 and W_1 were the weights of the sample before exposure to atmosphere and after equilibrium, respectively. The average value of three replicates for each sample was determined.

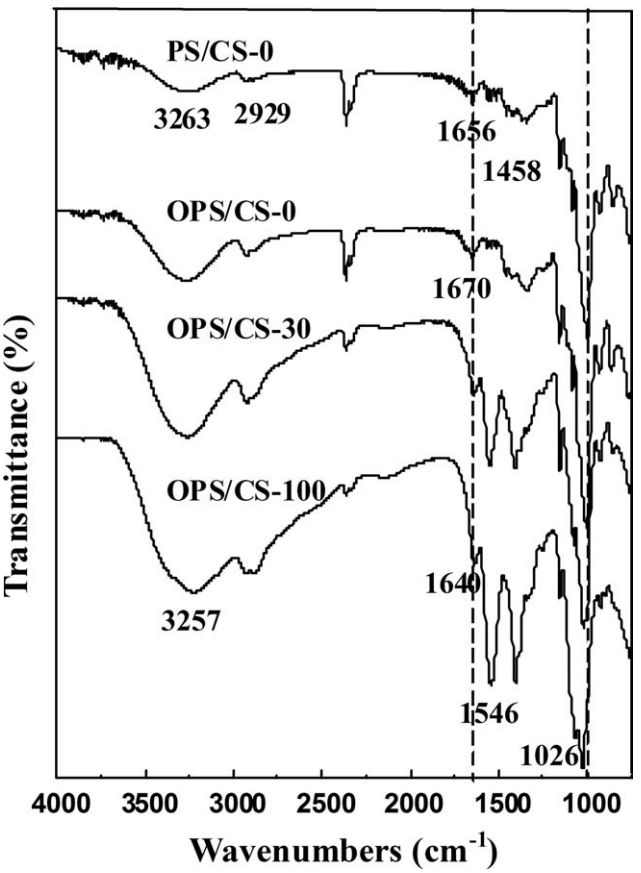

Figure 1 FTIR spectra of PS/CS-0, OPS/CS-0, OPS/CS-30, and OPS/CS-100 films.

RESULTS AND DISCUSSION

Fourier transform infrared spectroscopy

The FTIR spectra of PS/CS-0, OPS/CS-0, OPS/CS-30, and OPS/CS-100 films are presented in Figure 1. In the spectrum for starch (PS/CS-0), the broad band at 3263 cm^{-1} was due to OH stretching. The peak at 2929 cm^{-1} corresponded to C—H stretching, whereas the bands at 1656 cm^{-1} and 1458 cm^{-1} were assigned to the δ (O—H) bending of water and CH_2, respectively. The bands from 852 to 996 cm^{-1} corresponded to C—O bond stretching.[17] In the spectrum for oxidized starch (OPS/CS-0), the characteristic absorption peak for C=O stretching vibration was at about 1670 cm^{-1}, which overlapped the δ (O—H) bending of water. The band at 1656 cm^{-1} for OPS was stronger than that of PS, indicating that the hydroxyl groups in the C-6 positions of OPS were oxidized and that carboxyl groups had been introduced.[15] The CS spectrum (OPS/CS-100) was similar to that in the previous report of Mathew et al.[18] The broad band at 3257 cm^{-1} was due to OH stretching,

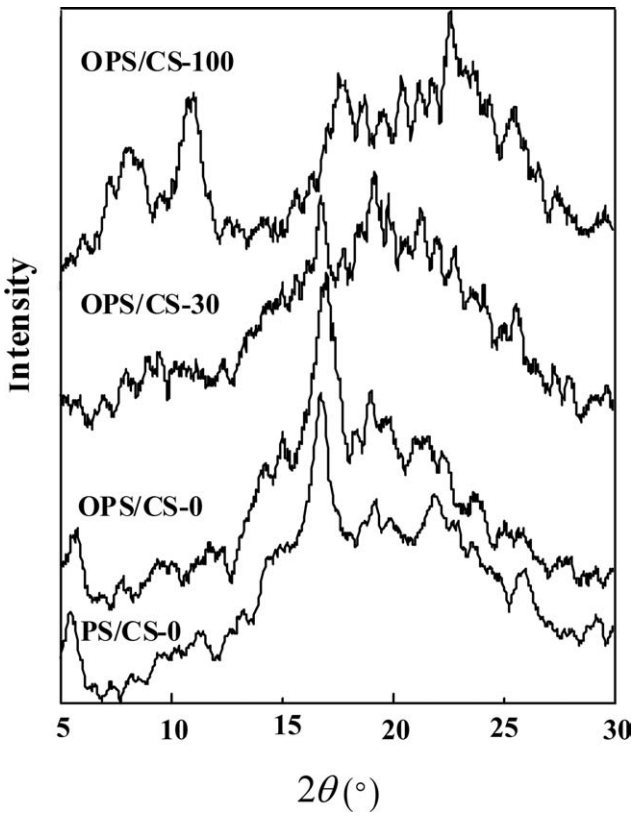

Figure 2 XRD patterns of PS/CS-0, OPS/CS-0, OPS/CS-30, and OPS/CS-100 films.

which overlapped the NH stretching in the same region. The band at 1546 cm^{-1} was due to NH bending (amide II). A small peak near 1640 cm^{-1} corresponded to C=O stretching vibrations (amide I) due to the residual amide of chitin in the CS matrix. The bands at 1026 cm^{-1} corresponded to C—O bond stretching.[17,18] Changes in characteristic spectra peaks may reflect how components are mixed/interacted, physically or chemically.[19,20] In this study, the peak for the hydroxyl groups could not be used to evaluate component interactions because of the interfering effects of from glycerol and water. Nevertheless, in the typical spectrum for a OPS/CS composite film, it was found that the C—O stretching vibration at 1026 cm^{-1} for CS had shifted to 996 cm^{-1} with the addition of OPS. This change can be attributed to hydrogen bonding and electrostatic interaction between oxidized starch and CS.

X-ray diffractometry

XRD patterns of PS/CS-0, OPS/CS-0, OPS/CS-30, and OPS/CS-100 films are shown in Figure 2. For the PS/CS-0 film, typical C-type crystallinity patterns with peaks at $2\theta = 5.70°$ (characteristic of B type polymorphs), 15.10° (characteristic of A type polymorphs), 17.21° (characteristic of both A and B type polymorphs), 20.18° and 22.58° (characteristic of B type polymorphs) were clearly observed and identical to published literature.[21] The OPS/CS-0 film showed an XRD pattern similar to that of the PS/CS-0 film. This indicated that the crystalline structure for starch was not altered by the oxidation reaction. This crystalline structure was ascribed to recrystallization or retrogradation of starch molecules after gelatinization and is similar to that often detected in starchy foods and thermoplastic materials.[22] Interestingly, the oxidized starch film (OPS/CS-0) exhibited higher angle diffraction peaks (2) than the neat starch film (PS/CS-0) showing that the d value decreased based on the Bragg formula ($2d \sin\theta = n\lambda$). This result implied that the polymer chains of oxidized starch exhibited even more compact packing due to the presence of newly introduced carboxyl groups after oxidization. The CS film (OPS/CS-100) was also in a crystalline state, as evidenced by the two main diffraction peaks ($2\theta = 11.60°$ and 20.25°) observed in its XRD pattern. This agreed with the finding reported by Nunthanid et al.[23]

Incorporation of CS had an effect on the crystalline structure of the OPS. Comparing the XRD patterns of OPS/CS-30 and OPS/CS-0, it was concluded that the crystalline peaks of OPS were suppressed. An amorphous hill was apparent accompanied by slightly weaker crystalline peaks, indicating a higher ratio of amorphous structure and lower crystallization, and proving that the stronger hydrogen bonding between oxidized starch and CS chains effectively prevented regular packing of the modified starch.[20]

Scanning electron microscopy

SEM micrographs of pea starch powder (a), OPS powder (b), and the fragile fractured surfaces of PS/CS-0 film (c), OPS/CS-0 film (d), OPS/CS-30 film (e), OPS/CS-100 film (f), PS/CS-30 film (g), and PS/CS-50 film (h) are shown in Figure 3. The SEM micrographs revealed that there was very little difference in the surface morphology and size of the native and oxidized field pea starches; granules were oval or spherical in shape and 20–40 μm in diameter. This was the same as the results for the hypochlorite oxidation of field pea starch reported by Li and Vasanthan.[24] Both neat PS film (PS/CS-0) and OPS film (OPS/CS-0) exhibited smooth cross-sections, though some granules were observed within the PS matrix. This may have resulted from recrystallization or retrogradation of PS molecules after gelatinization. The neat CS film (OPS/CS-100) exhibited a relatively smooth cross-section because of its good film-forming properties. Conversely, rough cross-sections in PS/CS-30 (g) and PS/CS-50 (h) films indicated that PS and CS were not quite

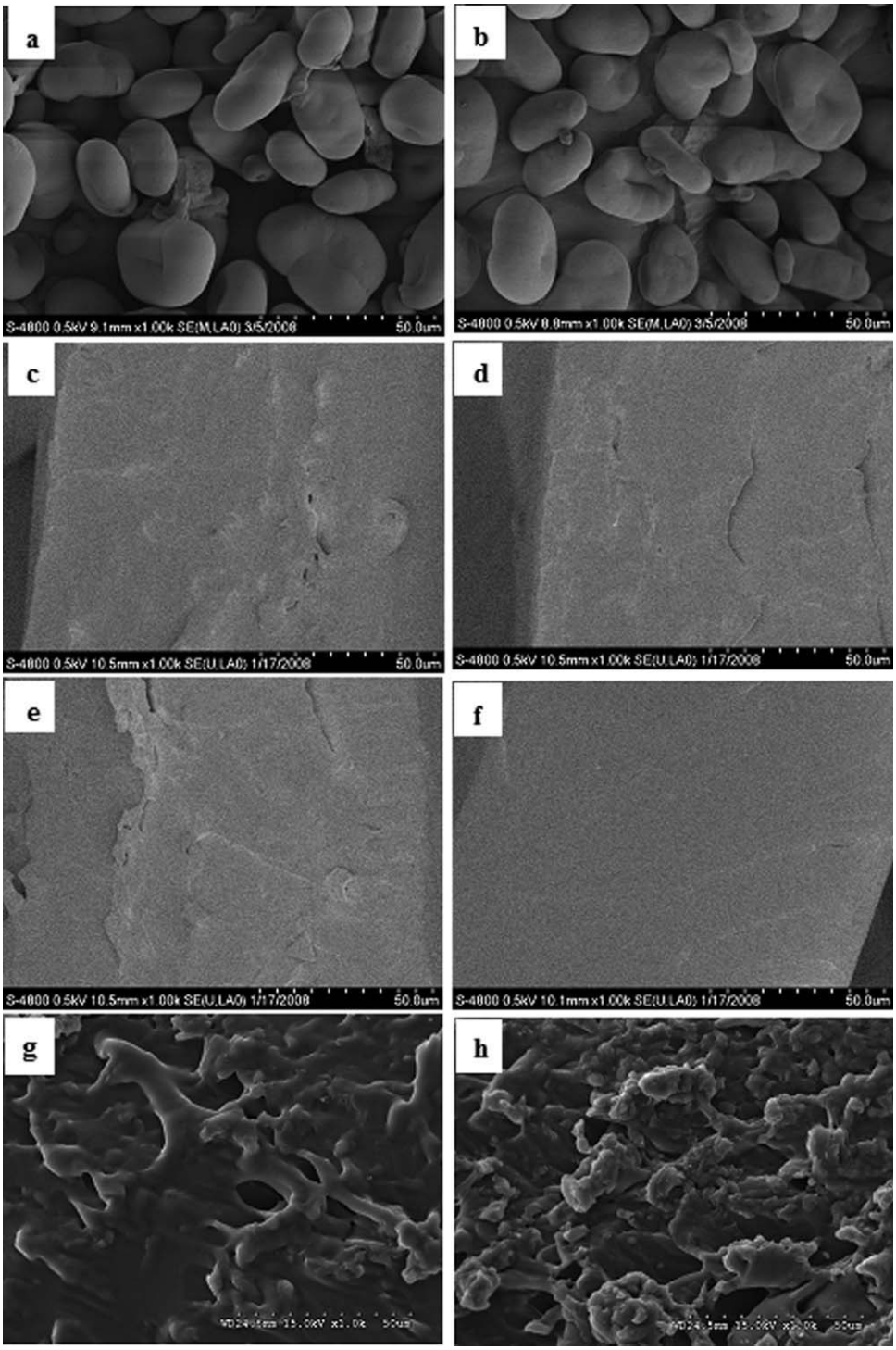

Figure 3 SEM micrographs of pea starch powders (a); OPS powders (b); fragile fractured surfaces of PS/CS-0 film (c); OPS/CS-0 film (d); OPS/CS-30 film (e); OPS/CS-100 film (f); PS/CS-30 film (g); and PS/CS-50 film (h). The scale bar is 50 μm.

compatible. It is worth mentioning that the cross-section of OPS/CS-30 was smoother (with no apparent phase separation) than that of PS/CS-30, which is an indication of the good compatibility between OPS and CS resulting from a strong electrostatic interaction between the OPS carboxyl and the amino groups of CS.[24]

Thermogravimetric and differential thermogravimetric analysis

The TG and DTG curves shown in Figure 4(a,b), respectively, were used to determine the weight loss of the material as it was heated. The initial weight loss of all samples, at ~ 50–100°C, was due to evaporation of water and solvent, whereas the weight

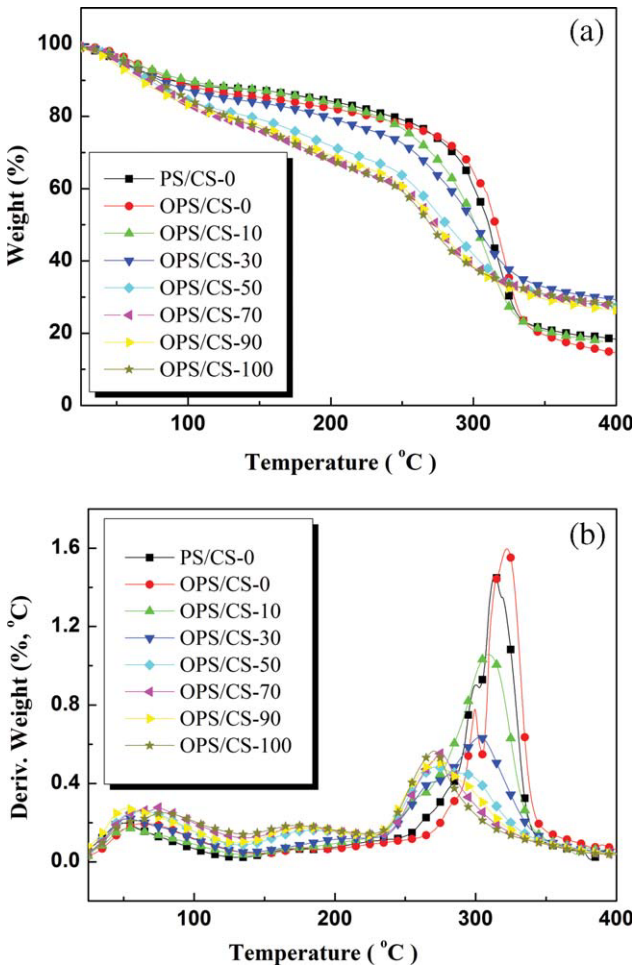

Figure 4 a) TG curves of PS/CS-0 and OPS/CS-*n* blend films and (b) DTG curves of PS/CS-0 and OPS/CS-*n* blend films. [Color figure can be viewed in the online issue, which is available at www.interscience.wiley.com.]

loss in the second range (250–350 °C) corresponded to a complex process including the dehydration of the saccharide rings and depolymerization.[25] The TG curves showed that all samples were stable up to 250°C. The temperatures of maximum loss ratio (T_{max}) for all samples are listed in Table II. When CS loading increased, the T_{max} of the blend films decreased, as observed in Figure 4(b), indicating that the thermostability of the oxidized starch-based films decreased with increased CS loading in the blend films. When CS loading was equal to or greater than 50%, the thermal decomposition temperature of the blend films was close to that of the CS film (OPS/CS-100).

Mechanical properties

Results for tensile strength and elongation at break of PS/CS (PS/CS-0 to PS/CS-100) and OPS/CS (from OPS/CS-0 to OPS/CS-100) composites are presented in Figures 5 and 6, respectively. Both the tensile strength (σ_b) and elongation at break (ε_b) of the OPS/CS films increased when the CS loading levels increased from 0 to 30 wt %. In the OPS/CS films where CS loading levels were greater than 30 wt %, tensile strength increased abruptly and elongation at break decreased. The OPS/CS-30 film exhibited the highest mechanical strength with a σ_b of 11.02 MPa and ε_b of 87.3%. The σ_b values of the OPS/CS-*n* films were higher than those of the PS/CS-*n* films, whereas the ε_b values were lower, indicating that oxidation introduced the carboxyl into the starch chain resulting in strong electrostatic and hydrogen bonding interactions between the OPS carboxyl and the CS amino groups. The strong interactions tend to decrease the motion of the chain segments and impair the recrystallization of starch, which explains why the tensile strength improved while the elongation at break decreased.

MU test

The MU at equilibrium at 92% RH is plotted in Figure 7 for the blend films with different CS contents. The MU value was determined by two opposite factors: interaction among components and the carboxyl group content. On one hand, the strong interaction between OPS and CS decreased the MU. On other hand, oxidation enhanced the water binding capacity of pea starch due to the introduction of hydrophilic groups into the native starch. It was observed that the MU value for the neat native starch (PS/CS-0) and the neat oxidized starch (OPS/CS-0) were 48.11 wt % and 41.02 %, respectively, indicating that oxidation treatment of starch reduced the MU. The MU values of OPS/CS blend films reached the minimum value of 29.52% when the CS loading was 10%. This indicated that OPS and CS formed strong interactions through hydrogen bonding and electrostatic interaction, inhibiting permeation of water molecules into the blend film, and thus decreasing the MU values. However, when CS loading was higher than 10 wt %, MU values for the blend films increased progressively, which may be due to an increase in hydroxyl groups as a result of CS incorporation.

TABLE II
Temperature of Maximum Weight Loss Ratio (T_{max}) for OPS/CS Blend Films Using Data Obtained from TGA Curves

Code	OPS/CS-0	OPS/CS-10	OPS/CS-30	OPS/CS-50	OPS/CS-70	OPS/CS-90	OPS/CS-100
T_{max}(°C)	317.3	311.3	301.4	271.3	275.2	277.1	276.8

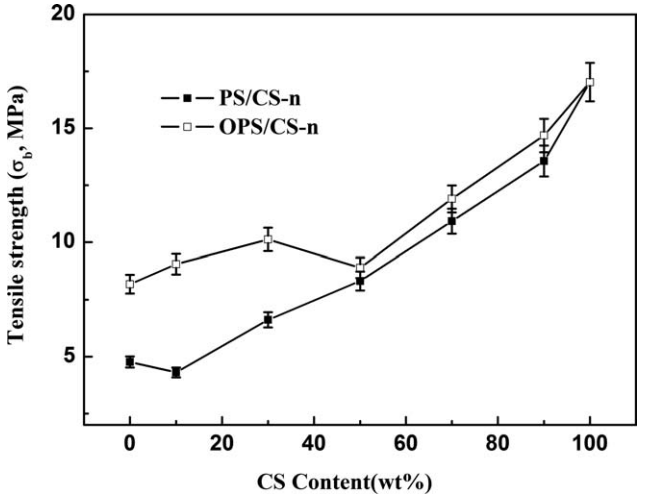

Figure 5 Tensile strength of OPS/CS-*n* and PS/CS-*n* blend films.

CONCLUSIONS

A series of composite films was prepared from glycerol-plasticized OPS and CS. Results from FTIR and XRD indicated that the strong interaction between OPS and CS resulted from strong hydrogen bonding and electrostatic interaction which resulted in good miscibility. Mechanical properties testing showed that the carboxyl groups introduced into the starch matrix improved the properties of the OPS/CS composites. The tensile strength of oxidized starch was higher than that of regular starch, and MU tests showed that the water barrier property of OPS blend films was improved. These all-natural, polysaccharide-based composites have potential applications in agriculture, drug release, and medicine, and in packaging fields as edible films, food packaging, and one-off packaging.

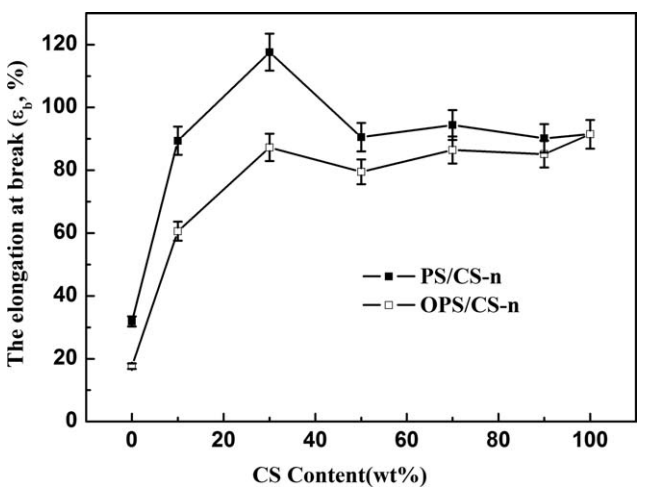

Figure 6 Elongation at break of OPS/CS-*n* and PS/CS-*n* blend films.

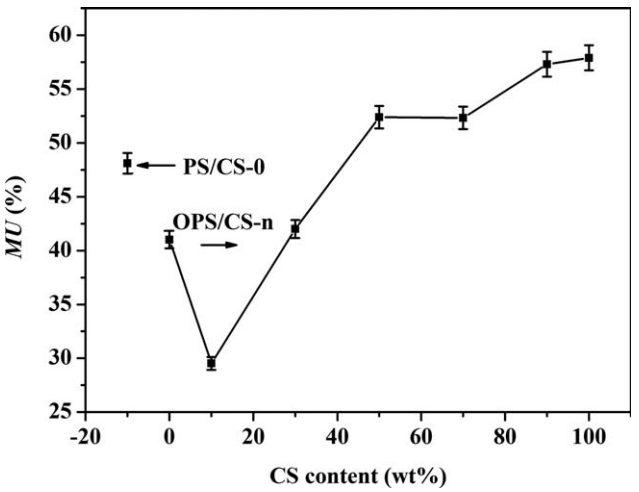

Figure 7 Moisture uptake at equilibrium of neat PS film and OPS/CS-*n* blend films conditioned at RH 92% as a function of CS content.

References

1. Cao, X.; Chen, Y.; Chang, P. R.; Stumborg, M.; Huneault, M. A. J Appl Polym Sci 2008, 109, 3804.
2. Huang, M. F.; Yu, J. G.; Ma, X. F.; Jin, P. Polymer 2005, 46, 3157.
3. Córdoba, A.; Cuéllar, N.; González, M.; Medina, J. Carbohydr Polym 2008, 73, 409.
4. Chillo, S.; Flores, S.; Mastromatteo, M.; Conte, A.; Gerschenson, L.; Del-Nobile, M. A. J Food Eng 2008, 88, 159.
5. Singh, J.; Kaur, L.; Mccarthy, O. J. Food Hydrocolloids 2007, 21, 1.
6. Patil, D. R.; Fanta, G. F.; Felker, F. C.; Salch, J. H. J Appl Polym Sci 2008, 108, 2749.
7. Jagannath, J. H.; Radhika, M.; Nanjappa, C.; Murali, H. S.; Bawa, A. S. J Appl Polym Sci 2006, 101, 3948.
8. Avella, M.; De Vliegar, J. J.; Errico, M. E.; Fischer, S.; Vacca, P.; Volpe, M. G. Food Chem 2005, 93, 467.
9. Szepes, A.; Makai, Z.; Blümer, C.; Mäder, K.; Kása P., JR.; Szabó-Révész, P. Carbohydr Polym 2008, 72, 571.
10. Martin, O.; Schwach, E.; Avérous, L.; Couturier, Y. Starch-Stärke 2001, 53, 372.
11. Mathew, S.; Abraham, T. E. Food Hydrocolloids 2008, 22, 826.
12. Wong, D. W. S.; Gastineau, F. A.; Gregorski, K. S.; Tillin, S. J.; Pavlath, A. E. J Agric Food Chem 1992, 40, 540.
13. Hoagland, P. D.; Parris, N. J Agric Food Chem 1996, 44, 1915.
14. Hosokawa, J.; Nishiyama, M.; Yoshihara, K.; Kubo, T. Ind Eng Chem Res 1990, 29, 800.
15. Huang, T. G.; Jiang, Q. M.; Zhang, B. L. Henan Chem Ind 2006, 23, 26.
16. Chattopadhyay, S.; Singhal, R. S.; Kulkarni, P. R. Carbohydr Polym 1997, 34, 203.
17. Xu, Y. X.; Kim, K. M.; Hanna, M. A.; Nag, D. Ind Crop Prod 2005, 21, 185.
18. Mathew, S.; Brahmakumar, M.; Abraham, T. E. Biopolymer 2006, 82, 176.
19. Guan, Y. L.; Liu, X. F.; Zhang, Y. P.; Yao, K. D. J Appl Polym Sci 1998, 67, 1965.
20. Yin, Y. J.; Yao, K. D.; Cheng, G. X.; Ma, J. B. Polym Int 1999, 48, 429.
21. Yoshimura, M.; Takaya, T.; Nishinari, K. Carbohydr Polym 1998, 35, 71.
22. Rindlav-Westling, A.; Stading, M.; Hermansson, A. M.; Gatenholm, P. Carbohydr Polym 1998, 36, 217.
23. Nunthanid, J.; Puttipipatkhachorn, S.; Yamamoto, K.; Peck, G. E. Drug Dev Ind Pharm 2001, 27, 143.
24. Li, J. H.; Vasanthan, T. Food Res Int 2003, 36, 381.
25. Mathew, A. P.; Dufresne, A. Biomacromolecules 2002, 3, 609.